



Article

# Structural Characterization of Core Region in *Erwinia amylovora* Lipopolysaccharide

Angela Casillo <sup>1</sup>, Marcello Ziaco <sup>1</sup>, Buko Lindner <sup>2</sup>, Susana Merino <sup>3</sup>, Elena Mendoza-Barberá <sup>3</sup>, Juan M. Tomás <sup>3</sup> and Maria Michela Corsaro <sup>1,\*</sup>

<sup>1</sup> Department of Chemical Sciences, University of Naples “Federico II”, Complesso Universitario Monte S. Angelo, Via Cintia 4, 80126 Naples, Italy; angela.casillo@unina.it (A.C.); marcello.ziaco@unina.it (M.Z.)

<sup>2</sup> Division of Bioanalytical Chemistry, Research Center Borstel, Leibniz-Center for Medicine and Biosciences, Parkallee 10, D-23845 Borstel, Germany; blindner@fz-borstel.de

<sup>3</sup> Department of Genética, Microbiología y Estadística, Universidad de Barcelona, Diagonal 643, 08071 Barcelona, Spain; smerino@ub.edu (S.M.); elenademendoza@hotmail.com (E.M.-B.); jtomás@ub.edu (J.M.T.)

\* Correspondence: corsaro@unina.it; Tel.: +39-081-674-149

Academic Editor: David Arráez-Román

Received: 2 February 2017; Accepted: 28 February 2017; Published: 4 March 2017

**Abstract:** *Erwinia amylovora* (*E. amylovora*) is the first bacterial plant pathogen described and demonstrated to cause fire blight, a devastating plant disease affecting a wide range of species including a wide variety of *Rosaceae*. In this study, we reported the lipopolysaccharide (LPS) core structure from *E. amylovora* strain CFBP1430, the first one for an *E. amylovora* highly pathogenic strain. The chemical characterization was performed on the mutants *waaL* (lacking only the O-antigen LPS with a complete LPS-core), *wabH* and *wabG* (outer-LPS core mutants). The LPSs were isolated from dry cells and analyzed by means of chemical and spectroscopic methods. In particular, they were subjected to a mild acid hydrolysis and/or a hydrazinolysis and investigated in detail by one and two dimensional Nuclear Magnetic Resonance (NMR) spectroscopy and ElectroSpray Ionization Fourier Transform-Ion Cyclotron Resonance (ESI FT-ICR) mass spectrometry.

**Keywords:** lipopolysaccharide; *Erwinia amylovora*; NMR; ESI FT-ICR; structural determination

## 1. Introduction

*Erwinia amylovora* is the causal agent of fire blight, a disease of nutritionally important members of the family *Rosaceae*, such as apple and pear trees. The symptoms in apple plants are present on rootstocks, blossoms, shoots, and fruits [1]. On fruits, the disease provokes the development of ooze, which is composed of bacteria, polysaccharides, and plant sap [1]. Bacteria are transported by insects, rain, birds, wind-wipping, and hail from the ooze to flowers. From flower infection, it can also be transferred to lateral parts of the plant through an endophytic mechanism [2].

Two major virulence determinants are known for the pathogenesis of *Erwinia*: (i) one involves the *hrp/dsp* gene cluster, the role of which is to secrete and deliver proteins from bacteria to plant apoplasts and cytoplasm [1]; (ii) the second is the production of two types of exopolysaccharides (EPS), amylovoran and levan [3,4].

The outer membrane (OM) of almost all Gram-negative bacteria and of some cyanobacteria [5–8] contains lipopolysaccharides (LPSs), where they constitute approximately 75% of the outer surface. They are amphiphilic endotoxic molecules necessary for the viability and survival of Gram-negative bacteria, as they seriously contribute to the structural integrity of the OM and to the protection of the bacterial cell envelope [9].

The colony morphology of Gram-negative bacteria can appear as smooth or rough as a consequence of a different structure of the lipopolysaccharides, named smooth (S-LPS) or rough (R-LPS), respectively. The structure of a S-LPS molecule can be described as three covalently linked domains: the glycolipid portion, called lipid A; the intermediate core oligosaccharide region (core); and the O-specific polysaccharide (O-chain) [10]. Instead, the R-LPSs (named lipooligosaccharides, LOSs) completely lacks the O-specific polysaccharide chain, either due to genetic mutation or to the inherent nature of bacteria [11].

Bacterial lipopolysaccharides show multiple roles in plant–microbe interactions. LPS give a contribution to the low permeability of the outer membrane, which acts as a barrier to protect microorganisms from plant-derived antimicrobial substances. LPS-defective mutants display augmented in vitro sensitivity to antibiotics and antimicrobial peptides and, upon introduction into susceptible plants, the numbers of viable bacteria often decay very quickly [12–14].

In this study we characterized the lipopolysaccharide core structure from the strain CFBP1430, the first one completely sequenced for a highly pathogenic *E. amylovora*. In particular, the results about *waaL*, *wabH*, and *wabG* mutants are reported. We studied *wabH* and *wabG* mutants because we found these genes in the *Erwinia amylovora* strain CFBP1430 *wb*; they were fully characterized in *Klebsiella pneumoniae* and *Serratia marcescens*, and both correspond to the outer-LPS core [15]. The lipooligosaccharides were degraded both by mild hydrazinolysis (O-deacylation) and hot KOH (N-deacylation). Both products were investigated by chemical analysis, by  $^1\text{H}$  and  $^{13}\text{C}$  NMR spectroscopy, and by ESI FT-ICR spectrometry.

## 2. Results and Discussion

### 2.1. Preparation and Structural Characterization of Oligosaccharides from *Ea* $\Delta$ *waaL* LPS

The LPSs from the *waaL*, *wabH*, and *wabG* mutants (*Ea* $\Delta$ *waaL*, *Ea* $\Delta$ *wabH*, and *Ea* $\Delta$ *wabG*, respectively) of the *Erwinia amylovora* strain CFBP1430 were extracted by the phenol-chloroform-light petroleum (PCP) method. *WabG* is responsible for the transfer of D-GalA to the O-3 position of L,D-Hep II, and *WabH* transfers a D-GlcNAc residue from UDP-GlcNAc to the D-GalA [15]. The monosaccharides composition was performed as already reported [16]. In particular, the Gas Chromatography-Mass Spectrometry (GC-MS) analysis of methyl and octyl glycosides for *Ea* $\Delta$ *waaL* and *Ea* $\Delta$ *wabH* mutant LPSs revealed the following sugars; D-Glc, D-GalA, D-GlcN, L,D-Hep, D,D-Hep, and Kdo. When this analysis was performed on *Ea* $\Delta$ *wabG* LPS, the lack of D-GalA and D,D-Hep was observed.

The removal of fatty acids from *Ea* $\Delta$ *waaL* LPS was performed both by strong alkaline and acetic acid hydrolyses. The obtained products were analyzed by ESI FT-ICR mass spectrometry. In addition, mono- and two-dimensional NMR spectroscopy ( $^1\text{H}$ ,  $^1\text{H}$  DQF-COSY,  $^1\text{H}$ ,  $^1\text{H}$  TOCSY,  $^1\text{H}$ ,  $^1\text{H}$  ROESY,  $^1\text{H}$ ,  $^{13}\text{C}$  HSQC-DEPT,  $^1\text{H}$ ,  $^{13}\text{C}$  HSQC-TOCSY, and  $^1\text{H}$ ,  $^{13}\text{C}$  HMBC) was allowed to assign all the proton and carbon chemical shifts of each mutant. The anomeric configurations were identified on the basis of both  $^{13}\text{C}$  chemical shift values and  $^3J_{\text{H}_1, \text{H}_2}$  coupling constants. The sequence of the residues in all the oligosaccharides was obtained both by long-range scalar couplings and by nuclear Overhauser enhancement (NOE) data.

Starting from the totally deacylated product (L-OS<sub>KOH</sub>, Scheme 1, structures 1a–c), the negative ion mode ESI FT-ICR mass spectrum of the sample identified eight main species (Figure 1 and Table 1). Species **M1**, occurring at 2220.595 Da (calculated molecular mass 2220.586 Da), represented the higher molecular mass oligosaccharide chain containing the phosphorylated lipid A backbone and the core structure.



or more sugars from GalA, due to a  $\beta$ -elimination reaction [17]. Species **M3**, **M5**, and **M8** differed from **M1** in their heptoses composition, displaying four units in **M3** and three and two in **M5** and **M8**, respectively. The remaining species, **M2**, **M4**, and **M7**, lacked a glucose unit respect to **M1**, **M3**, and **M5**, respectively, thus confirming the terminal position for this residue, while the **M6** species lacked  $\Delta$ GalA compared to **M5**. Further mass peaks originate from an additional phosphate group P ( $\Delta m = +79.966$  u) and/or one linked C14:0(3OH) fatty acid ( $\Delta m = +226.193$  u) due to incomplete deacylation. Finally, **F1–F6** are fragments induced during the ESI process leading to the cleavage of the lipid A backbone GlcN<sub>2</sub>P<sub>2</sub> ( $\Delta m = -500.081$  u).

Despite the complexity of the <sup>1</sup>H-<sup>13</sup>C Heteronuclear Single Quantum Coherence-Distortionless Enhancement by Polarization Transfer (HSQC-DEPT) experiment (Figure 2), it was possible to assign the signals of the main species, **M1**, **M3**, and **M5**. All the NMR data (Table 2, structures 1a–c) strongly suggested that the fractions L-OS<sub>KOH</sub> and the structure of the oligosaccharide OS1 obtained from the previously published *K. pneumoniae* 52145 *waaL* mutant [17] possessed a common structural element constituted by the residues **A**, **B**, **C**, **D**, **E**, **F**, **G**, **H**, and **I** (monosaccharide units are as shown in Table 2), in agreement with the strain genomics.

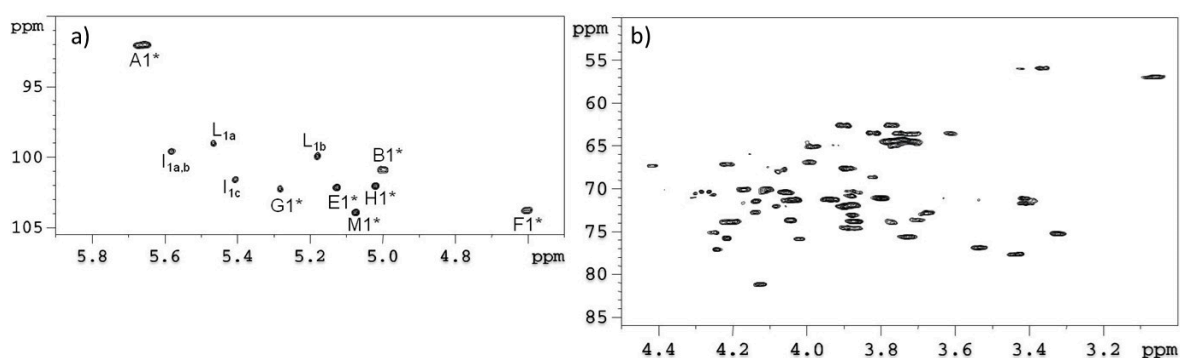


**Figure 2.** Anomeric (a) and carbinolic (b) region of <sup>1</sup>H-<sup>13</sup>C HSQC-DEPT of the totally deacylated LPS (L-OS<sub>KOH</sub>) from *E. amylovora waaL* mutant. All the correlation cross-peaks in the anomeric region indicate the signals of structures 1a–c. The spectrum was recorded in D<sub>2</sub>O at 298 K at 600 MHz.

**Table 2.** <sup>1</sup>H and <sup>13</sup>C chemical shifts ( $\delta$ ) of sugar residues of core oligosaccharides from *Erwinia amylovora* LPS. Nuclear Magnetic Resonance (NMR) spectra were recorded in D<sub>2</sub>O at 600 MHz at 298 K.

Residue	Nucleus	H1	H2	H3	H4	H5	H6	H7	H8
		C1	C2	C3	C4	C5	C6	C7	C8
$\alpha$ -GlcN1P A, 1a–c	<sup>1</sup> H	5.65	3.37	3.94	3.41	4.21	3.88/4.27		
	<sup>13</sup> C	92.0	55.9	71.2	71.1	73.8	70.2		
$\alpha$ -GlcN1P A, 3	<sup>1</sup> H	5.53	3.28	3.80	3.51	4.05	3.65/4.20		
	<sup>13</sup> C	92.0	55.9	71.0	70.9	73.4	71.0		
$\alpha$ -GlcN1P A, 4	<sup>1</sup> H	5.54	3.30	3.80	3.51	4.04	3.65/4.19		
	<sup>13</sup> C	92.0	57.1	71.0	71.1	73.6	71.3		
$\beta$ -GlcN4P B, 1a–c	<sup>1</sup> H	4.99	3.06	3.88	3.88	3.72	3.62/3.75		
	<sup>13</sup> C	100.9	56.9	73.1	74.6	75.6	63.5		
$\beta$ -GlcN4P B, 3	<sup>1</sup> H	4.72	2.93	3.73	3.72	3.60	3.35/3.57		
	<sup>13</sup> C	100.9	56.9	70.9	74.0	72.3	63.7		
$\beta$ -GlcN4P B, 4	<sup>1</sup> H	4.73	2.94	3.72	3.73	3.63	3.35/3.60		
	<sup>13</sup> C	100.9	57.1	70.9	73.8	75.3	64.0		
4,5-Kdo C, 1a–c	<sup>1</sup> H	n.d.	n.d.	1.88/2.12	4.21	4.21	4.14	4.17	3.77/3.92
	<sup>13</sup> C	n.d.	n.d.	36.0	73.9	75.7	72.9	70.2	64.9
4,5-Kdo C, 3	<sup>1</sup> H	175.6	100.7	1.81/1.98	4.03	4.17	3.83	3.51	3.62–3.87
	<sup>13</sup> C	175.6	100.7	36.0	71.6	70.1	74.0	73.4	64.3

Table 2. Cont.

Residue	Nucleus	H1	H2	H3	H4	H5	H6	H7	H8
		C1	C2	C3	C4	C5	C6	C7	C8
4,5-Kdo C, 4	<sup>1</sup> H	176.3	101.1	1.88/2.04	3.99	4.17	3.88	3.54	3.61-3.87
	<sup>13</sup> C			36.2	72.0	70.4	71.9	73.6	64.7
t-Kdo D, 1a-c	<sup>1</sup> H	n.d.	n.d.	1.82/2.18	4.09	4.06	3.71	4.09	3.77/3.99
	<sup>13</sup> C			35.9	68.1	67.7	73.7	72.1	65.0
t-Kdo D, 3	<sup>1</sup> H	176.1	102.6	1.67/2.06	3.95	3.95	3.60	3.56	3.56/3.87
	<sup>13</sup> C			35.7	67.4	67.4	73.9	73.1	64.5
t-Kdo D, 4	<sup>1</sup> H	176.1	102.8	1.66/2.00	3.96	3.94	3.62	3.56	3.61/3.78
	<sup>13</sup> C			36.3	67.7	67.9	73.3	73.3	65.1
3,4- $\alpha$ -L,D-Hep E, 1a-c	<sup>1</sup> H	5.12	4.13	4.24	4.25	4.10	4.17	3.76	
	<sup>13</sup> C			102.2	71.5	77.1	75.1	70.1	70.2
3,4- $\alpha$ -L,D-Hep E, 2a,b	<sup>1</sup> H	5.12	4.07	4.23	4.23	4.10	4.15	3.75	
	<sup>13</sup> C			101.9	71.4	77.1	75.3	70.3	69.8
3,4- $\alpha$ -L,D-Hep E, 3	<sup>1</sup> H	5.19	3.95	4.06	4.19	4.18	4.00	3.69	
	<sup>13</sup> C			100.1	71.8	75.1	74.4	72.2	70.2
3,4- $\alpha$ -L,D-Hep E, 4	<sup>1</sup> H	5.16	4.00	3.99	4.15	4.12	3.98	3.68/3.89	
	<sup>13</sup> C			103.0	72.0	75.6	74.6	73.3	70.3
t- $\beta$ -Glc F, 1a-c	<sup>1</sup> H	4.60	3.33	3.53	3.41	3.42	3.77/3.90		
	<sup>13</sup> C			103.8	75.3	77.0	71.7	77.7	62.5
t- $\beta$ -Glc F, 2a,b	<sup>1</sup> H	4.62	3.31	3.54	3.41	3.42	3.77/3.90		
	<sup>13</sup> C			104.0	75.3	77.0	71.1	77.5	62.5
t- $\beta$ -Glc F, 3	<sup>1</sup> H	4.46	3.18	3.41	3.26	3.30	3.63/3.78		
	<sup>13</sup> C			103.2	75.0	76.5	71.1	77.3	62.7
t- $\beta$ -Glc F, 4	<sup>1</sup> H	4.43	3.19	3.39	3.23	3.36	3.61-3.85		
	<sup>13</sup> C			103.6	75.0	76.9	71.6	77.8	62.8
3,7- $\alpha$ -L,D-Hep G, 1a-c	<sup>1</sup> H	5.28	4.26	4.13	3.99	3.78	4.21	3.80	
	<sup>13</sup> C			102.1	70.8	81.1	66.9	74.0	67.1
3,7- $\alpha$ -L,D-Hep G, 2a,b	<sup>1</sup> H	5.26	4.12	4.03	4.01	3.90	4.17	3.77	
	<sup>13</sup> C			102.0	71.1	80.8	66.9	74.0	71.1
3,7- $\alpha$ -L,D-Hep G, 3	<sup>1</sup> H	5.27	4.08	3.89	3.83	3.92	n.d.	3.69	
	<sup>13</sup> C			102.2	70.7	80.6	66.9	73.3	n.d.
t- $\alpha$ -L,D-Hep G, 4	<sup>1</sup> H	5.16	4.06	3.77	3.77	3.56	3.95	3.55	
	<sup>13</sup> C			100.1	71.0	72.0	67.6	73.2	70.3
t- $\alpha$ -L,D-Hep H, 1a-c	<sup>1</sup> H	5.02	4.04	3.90	3.89	3.67	4.06	3.72	
	<sup>13</sup> C			102.0	73.6	70.9	67.6	72.9	70.5
t- $\alpha$ -L,D-Hep H, 2a,b	<sup>1</sup> H	4.94	4.02	4.02	3.87	3.64	n.d.	n.d.	
	<sup>13</sup> C			101.8	73.1	71.3	67.6	72.7	n.d.
t- $\alpha$ -L,D-Hep H, 3	<sup>1</sup> H	4.84	3.88	3.91	3.88	3.63	3.93	3.64	
	<sup>13</sup> C			102.9	71.3	70.3	67.0	73.4	64.6
2- $\Delta$ -GalA I, 1a,b	<sup>1</sup> H	5.58	4.02	4.53	5.82				
	<sup>13</sup> C			99.6	75.8	65.8	108.9		
t- $\Delta$ -GalA I, 1c	<sup>1</sup> H	5.40	3.87	4.42	n.d.				
	<sup>13</sup> C			101.6	71.9	67.3	n.d.		
2,4- $\alpha$ -GalA I, 2a,b	<sup>1</sup> H	5.48	4.07	4.22	4.23	4.47			
	<sup>13</sup> C			99.5	80.4	68.5	77.2	72.6	176.2
2- $\alpha$ -GalA I, 3	<sup>1</sup> H	5.39	3.91	3.96	4.21	4.34			
	<sup>13</sup> C			98.9	80.6	69.2	72.2	73.7	176.8
2- $\alpha$ -D,D-Hep L, 1a	<sup>1</sup> H	5.35	4.06	3.97	3.89	n.d.	4.12	3.61	
	<sup>13</sup> C			98.9	80.0	71.4	68.5	n.d.	72.1

Table 2. Cont.

Residue	Nucleus	H1	H2	H3	H4	H5	H6	H7	H8
		C1	C2	C3	C4	C5	C6	C7	C8
t- $\alpha$ -D,D-Hep L, 1b	$^1\text{H}$	5.18	4.03	3.90	3.83	3.87	4.04	3.82	
	$^{13}\text{C}$	99.9	71.3	72.1	68.7	73.9	71.4	63.5	
2- $\alpha$ -D,D-Hep L, 2a,b	$^1\text{H}$	5.28	3.99	3.99	3.81	3.99	4.05	3.84	
	$^{13}\text{C}$	96.9	80.8	71.4	68.9	75.0	71.4	63.6	
2- $\alpha$ -D,D-Hep L, 3	$^1\text{H}$	4.99	3.87	3.75	3.67	3.92	4.09	3.69	
	$^{13}\text{C}$	98.3	80.6	71.7	68.7	73.3	73.1	63.1	
t- $\alpha$ -L,D-Hep M, 1a	$^1\text{H}$	5.09	4.07	4.07	3.88	3.70	n.d.	n.d.	
	$^{13}\text{C}$	103.5	71.3	73.7	67.7	73.1	n.d.	n.d.	
t- $\alpha$ -L,D-Hep M, 2a,b	$^1\text{H}$	5.05	4.05	4.06	3.86	n.d.	n.d.	n.d.	
	$^{13}\text{C}$	103.5	71.4	73.8	67.7	n.d.	n.d.	n.d.	
t- $\alpha$ -L,D-Hep M, 3	$^1\text{H}$	5.21	3.89	3.75	3.83	4.18	n.d.	3.56/3.78	
	$^{13}\text{C}$	101.9	71.5	70.1	66.8	72.1	n.d.	64.8	
4- $\alpha$ -GlcN N, 2a,b	$^1\text{H}$	5.19	3.27	3.85	3.79	4.17	3.83		
	$^{13}\text{C}$	97.6	55.3	72.5	77.0	72.5	61.3		
6- $\alpha$ -Glc O, 2a,b	$^1\text{H}$	5.49	3.62	3.74	3.90	3.54	3.88/4.20		
	$^{13}\text{C}$	100.7	72.8	74.2	73.0	70.8	69.8		
t- $\beta$ -Glc P, 2a	$^1\text{H}$	4.50	3.33	3.51	3.42	3.47	3.74/3.92		
	$^{13}\text{C}$	103.9	74.5	77.0	71.0	77.3	62.3		
2- $\beta$ -Glc P, 2b	$^1\text{H}$	4.62	4.47	3.59	3.45	3.46	3.74/3.92		
	$^{13}\text{C}$	103.9	78.9	75.9	70.9	77.3	62.3		
t- $\beta$ -Glc Q, 2b	$^1\text{H}$	4.36	3.61	3.75	3.47	4.17	n.d.		
	$^{13}\text{C}$	99.2	72.9	74.2	70.8	72.9	n.d.		

All the species possessed  $\alpha$ -GlcN1P residue at the reducing end (**A**, H1,  $\delta$  5.65 ppm; C1,  $\delta$  92.0 ppm), originating from the lipid A backbone. The second residue of glucosamine of the lipid A (**B**, H1,  $\delta$  4.99 ppm, C1,  $\delta$  100.9 ppm) was O-4 phosphorylated, as suggested by the downfield shift of both H4 and C4 chemical shifts [18]. In all the oligosaccharides corresponding to the **M1–M7** species, the core region was linked to the lipid A backbone through an  $\alpha$ -Kdo residue **C**, which was substituted at O-4 position by a second residue of Kdo (**D**).

Residues **E**, **G**, **H**, **L**, and **M** were identified as five *manno*-configured  $\alpha$ -heptopyranoses due to their small coupling constants  $^3J_{\text{H1,H2}}$  and  $^3J_{\text{H2,H3}}$  values. Downfield shifted carbon signals with respect to reference values [19] indicated substitutions at O-3 and O-4 of residue **E** (C3 at 77.1 and C4 at 75.1 ppm, respectively) and at O-3 and O-7 of residue **G** (C3 at 81.1 ppm and C7 at 71.2 ppm). Both residues **H** and **M** were identified as terminal units as none of their carbon signals were downfield shifted. All the heptose residues were found to be *L,D*-configured except for **L**; in fact, for this residue, the chemical shift of its C6 at 72.1 ppm suggested a *D,D*-configuration [20]. In addition, the downfield shift of its C2 resonance at 80.0 ppm clearly indicated that it was substituted at this position. Residue **I**, with H1/C1 at 5.58/99.6 ppm and H4/C4 at 5.82/108.9 ppm, was identified as a  $\alpha$ -threo-hex-4-enuronopyranosyl unit ( $\Delta$ GalA).

Finally, residue **F** was assigned to a  $\beta$ -glucose residue, on the basis of the proton multiplicities obtained by the DQF-COSY and TOCSY experiments. No downfield carbon chemical shifts were observed for this residue, thus indicating its terminal non reducing end position.

The sequence of the residues was deduced from the HMBC experiment, which showed correlations between C1 of **L** and H2 of **I**, H1 of **I** and C3 of **G**, H1 of **G** and C3 of **E**, C1 of **H** and H7 of **G**, and C1 of **F** and H4 of **E**.

In addition, residue **M** was found to be linked at the O-2 position of residue **L**, as shown by NOE contacts among H1 of **M** and both H1 and H2 of **L**, observed in the ROESY experiment. This last completed and confirmed the above sequence by inter-residual dipolar couplings. In the same



**Table 3.** Composition of the main species observed in the charge deconvoluted ESI FT-ICR mass spectrum of supernatant of the acetic acid hydrolysed LPS fraction (L-OS<sub>AcOH</sub>) isolated from *E. amylovora waa* L. mutant.

Species	Observed Mass (Da)	Calculated Mass (Da)	Composition
N1	2183.699	2183.698	Kdo <sub>1</sub> Hep <sub>5</sub> Glc <sub>4</sub> GalA <sub>1</sub> GlcN <sub>1</sub>
N2	2021.646	2021.645	Kdo <sub>1</sub> Hep <sub>5</sub> Glc <sub>3</sub> GalA <sub>1</sub> GlcN <sub>1</sub>
N3	1991.632	1991.635	Kdo <sub>1</sub> Hep <sub>4</sub> Glc <sub>4</sub> GalA <sub>1</sub> GlcN <sub>1</sub>
N4	1859.597	1859.592	Kdo <sub>1</sub> Hep <sub>5</sub> Glc <sub>2</sub> GalA <sub>1</sub> GlcN <sub>1</sub>
N5	1829.590	1829.578	Kdo <sub>1</sub> Hep <sub>4</sub> Glc <sub>3</sub> GalA <sub>1</sub> GlcN <sub>1</sub>
N6	1667.541	1667.529	Kdo <sub>1</sub> Hep <sub>4</sub> Glc <sub>2</sub> GalA <sub>1</sub> GlcN <sub>1</sub>
N7	1637.527	1637.518	Kdo <sub>1</sub> Hep <sub>3</sub> Glc <sub>3</sub> GalA <sub>1</sub> GlcN <sub>1</sub>
N8	1475.476	1475.466	Kdo <sub>1</sub> Hep <sub>3</sub> Glc <sub>2</sub> GalA <sub>1</sub> GlcN <sub>1</sub>

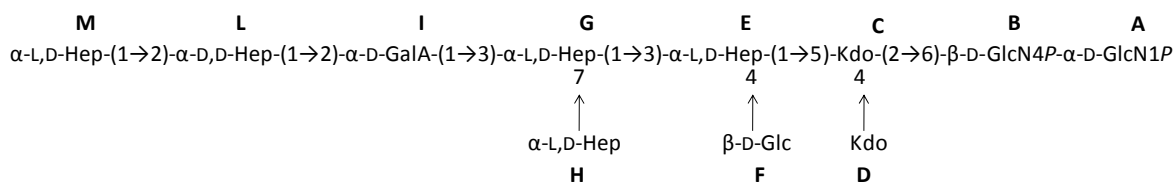
We compared our NMR data with the data already published for deacylated oligosaccharides from *Serratia marcescens* [19], and we found very similar chemical shifts, even if we recognized in *Erwinia* an additional minor component (N1 species, Table 2 and Figure 3). In fact, the molecular mass of the N1 species indicated an additional hexose with respect to that of N2. This residue (Q, Table 2) was identified as gluco-configured with an  $\alpha$  anomeric configuration, as suggested by its  $^3J_{H1,H2}$  anomeric coupling constant of 3.5 Hz. A long-range heteronuclear scalar coupling between H1 of Q and C2 of P indicated that in the N1 species the oligosaccharide substituting the O-4 of GalA had the structure:  $\alpha$ -Glc-(1  $\rightarrow$  2)- $\beta$ -Glc-(1  $\rightarrow$  6)- $\alpha$ -Glc-(1  $\rightarrow$  4)- $\alpha$ -GlcN. All these data were in agreement with the methylation analysis, except for the 2,4-disubstituted galacturonic acid residue, which was absent in the GC-MS chromatogram. This fact could be due to the hindrance of both oligosaccharides substituting O-2 and O-4 positions of GalA, thus preventing its methylation.

## 2.2. Preparation and Structural Characterization of Oligosaccharides from *Ea* $\Delta$ wabH and *Ea* $\Delta$ wabG LPSs

The LPSs from *Ea* $\Delta$ wabH and *Ea* $\Delta$ wabG mutants were completely deacylated by hydrazine followed by the KOH reaction. After purification on a gel filtration Sephadex G10 column, the samples, named H-OS<sub>KOH</sub> and G-OS<sub>KOH</sub> respectively, were analysed by mono- and two-dimensional NMR experiments (Table 2). The acetic acid hydrolysis was not performed on these two mutants as no  $\beta$ -degradation was observed for these samples, indicating that no information was lost.

The  $^1H$  NMR spectrum of the totally deacylated *Ea* $\Delta$ wabH LPS (H-OS<sub>KOH</sub>, Figure S1, Supporting Information) showed nine main anomeric proton signals, assigned to residues A–M, in the range 5.6–4.4 ppm. Signals in the range 2.2–1.5 ppm, attributable to the presence of the Kdo units, were also present.

The galacturonic acid residue (residue I, Scheme 3, structure 3) was recognized from the chemical shift of its C6 at  $\delta$  176.8 ppm (Table 2), which correlated with its H5 proton at  $\delta$  4.34 ppm in the Heteronuclear Multiple Bond Correlation (HMBC) experiment.



**Scheme 3.** Structures of the totally deacylated LPS fraction (H-OS<sub>KOH</sub>) isolated from the *E. amylovora* *Ea* $\Delta$ wabH mutant.

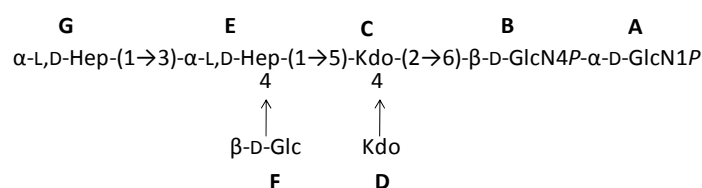
In addition, the O-substitution at position 2 of I was inferred by the long-range between H1 of L and C2 of I. The value of the coupling constant  $^3J_{H1,H2}$  of the anomeric proton was found to be 3.5 Hz, thus indicating for residue I an  $\alpha$  configuration. The chemical shifts of heptoses E, G, H, L, and M



were in agreement with that already found for structure **1**, as well as that of terminal  $\beta$ -Glc **F**. Finally, both the HMBC (Figure S2) and ROESY experiments indicated the sequence shown in structure **3**, which is in agreement with strain genomics.

The  $^1\text{H}$ -NMR spectrum of the totally deacylated Ea $\Delta$ wabG LPS, (G-OS<sub>KOH</sub>, Figure S3, Supporting Information) showed only five anomeric proton signals. All the  $^1\text{H}$  and  $^{13}\text{C}$  chemical shifts of each residue were identified and assigned by two-dimensional NMR experiments (Table 2). NMR data, together with glycosyl analysis, indicated the lack of the trisaccharide  $\alpha$ -Hep-(1  $\rightarrow$  2)- $\alpha$ -Hep-(1  $\rightarrow$  2)- $\alpha$ -GalA. This was in agreement with the hypothesis of assignment of the *wabG* gene to a galacturonic acid residue glycosyltransferase. In addition, the  $^1\text{H}$ ,  $^{13}\text{C}$  HSQC-DEPT NMR experiment (Figure S4) revealed the absence of the inner core heptose residue **H**, since only two L,D-heptose anomeric signals, **E** and **G**, were found (Scheme 4, structure 4).

This fact suggested that the lack of GalA residue may preclude the addition of heptose **H** to the position O-7 of heptose **G**.



**Scheme 4.** Structures of the totally deacylated LPS fraction (G-OS<sub>KOH</sub>) isolated from the *E. amylovora* Ea $\Delta$ wabG mutant.

### 3. Experimental Section

#### 3.1. Bacteria Growth and LPS Isolation

Dried bacteria cells from Ea $\Delta$ waaL (3.3 g), Ea $\Delta$ wabH (2.63 g), and Ea $\Delta$ wabG (3.58 g) mutants of *E. amylovora* strain CFBP1430 were all extracted by the PCP method [21] to give 208 mg of LPS (LPS<sub>PCP</sub> yield 6.3% *w/w* of dried cells) for the *waaL* mutant, 124 mg of LPS for the *wabH* mutant (LPS<sub>PCP</sub> yield 4.2% *w/w* of dried cells), and 170 mg of LPS (LPS<sub>PCP</sub> yield 4.7% *w/w* of dried cells) for the *wabG* mutant, respectively.

#### 3.2. Sugar Analysis

The sugar analysis was performed as reported [16]. The absolute configurations of the sugars were determined by gas chromatography of the acetylated (S)-2-octyl glycosides [22]. The derivatized samples were injected into an Agilent Technologies gas chromatograph 6850A equipped with a mass selective detector 5973N and a Zebron ZB-5 capillary column (Phenomenex, Bologna, Italy, 30 m  $\times$  0.25 mm i.d., flow rate 1 mL/min, He as carrier gas). The following temperature programs were used; 140  $^{\circ}\text{C}$  for 3 min, 140  $^{\circ}\text{C}$   $\rightarrow$  240  $^{\circ}\text{C}$  at 3  $^{\circ}\text{C}/\text{min}$  (acetylated methyl glycosides), 150  $^{\circ}\text{C}$  for 5 min, 150  $^{\circ}\text{C}$   $\rightarrow$  240  $^{\circ}\text{C}$  at 6  $^{\circ}\text{C}/\text{min}$ , and 240  $^{\circ}\text{C}$  for 5 min (acetylated octyl glycosides).

#### 3.3. Mild Acid Hydrolysis

The LPS of the Ea $\Delta$ waaL mutant (20 mg) was treated with 5% aqueous CH<sub>3</sub>COOH (2 mL, 100  $^{\circ}\text{C}$  for 4 h). After centrifugation (7500 rpm, 4  $^{\circ}\text{C}$ , 30 min), the pellet was washed twice with water. Then, the supernatant layers were pooled together and lyophilized. The sample was then fractionated on a Bio-Gel P-10 column (Biorad, 1.5  $\times$  110 cm, flow rate 15 mL/h, fraction volume 2 mL) and eluted with water buffered with 0.05 M pyridine and 0.05 M AcOH. The fractions containing oligosaccharides were pooled and named L-OS<sub>AcOH</sub> (10.1 mg).

### 3.4. Deacylation of the LOSs

The LOS from each mutant (100 mg) was dried over phosphorus anhydride under a vacuum and treated with hydrazine (5 mL, at 37 °C for 2 h) [23]. Cold acetone was added, and the pellet was recovered after centrifugation at 4 °C and 7000 rpm for 30 min. After being washed three times with acetone, it was suspended in water and lyophilized, obtaining L<sub>LOS-OH</sub> (68.6 mg), H<sub>LOS-OH</sub> (72.4 mg), and G<sub>LOS-OH</sub> (65.9 mg).

The partially deacylated LPS (LOS-OH) from each mutant was dissolved in KOH 4 M and incubated at 120 °C for 16 h. The KOH was neutralized with HCl, and the mixture was extracted three times with CHCl<sub>3</sub>. The aqueous phases were recovered and desalted on a Sephadex G-10 column (Amersham Biosciences, Little Chalfont, UK, 2.5 × 43 cm, 31 mL·h<sup>-1</sup>, fraction volume 2.5 mL, eluent NH<sub>4</sub>HCO<sub>3</sub> 10 mM). The eluted oligosaccharides mixture was then lyophilized (L-OS<sub>KOH</sub> 19 mg; H-OS<sub>KOH</sub> 13 mg; G-OS<sub>KOH</sub> 20 mg).

### 3.5. Methylation Analysis

The linkage positions of the monosaccharides were determined by GC-MS analysis of the partially methylated alditol acetates (PMAAs). The acetic acid oligosaccharides fraction of EaΔwaaL mutant (1 mg) was first reduced with NaBD<sub>4</sub> and then methylated with CH<sub>3</sub>I (100 μL) and NaOH powder in dimethyl sulfoxide (DMSO) (300 μL) for 20 h [24].

The reduction of the carboxymethyl groups was obtained by treating the sample with sodium boro deuteride (NaBD<sub>4</sub>). After the reaction working up, the sample was totally hydrolyzed with 2 M trifluoroacetic acid (TFA) at 120 °C for 2 h, reduced again with NaBD<sub>4</sub>, and acetylated with Ac<sub>2</sub>O and pyridine (50 μL each, 100 °C for 30 min) [25]. The PMAA mixture was analyzed by GC-MS with the following temperature program: 90 °C for 1 min, 90 → 140 °C at 25 °C/min, 140 °C → 200 °C at 5 °C/min, 200 → 280 °C at 10 °C/min, and 280 °C for 10 min.

### 3.6. Mass Spectrometry Analysis

Mass spectra were (ESI FT-ICR) were performed in negative ion mode using an APEX QE (Bruker Daltonics GmbH, Bremen, Germany) equipped with a 7 Tesla actively shielded magnet. The sample concentration was ~10 ng/μL. The solutions were sprayed at a flow rate of 2 μL/min and analyzed. The mass spectra obtained were charge-deconvoluted, and the mass numbers reported refer to the monoisotopic masses of the neutral molecules.

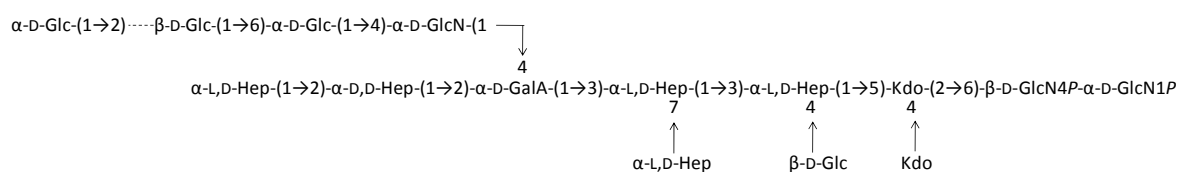
### 3.7. NMR Spectroscopy

<sup>1</sup>H and <sup>13</sup>C NMR spectra were performed using a Bruker Avance 600 MHz spectrometer (Milano, Italy) equipped with a cryoprobe. All 2D homo- and heteronuclear experiments (double quantum-filtered correlation spectroscopy, DQF-COSY; total correlation spectroscopy TOCSY; rotating-frame nuclear Overhauser enhancement spectroscopy, ROESY; nuclear Overhauser effect spectroscopy, <sup>1</sup>H,<sup>13</sup>C HSQC-DEPT; and heteronuclear multiple bond correlation, <sup>1</sup>H,<sup>13</sup>C HMBC) were obtained using the standard pulse sequences available in the Bruker software (TopSpin 3.1 version). The TOCSY and ROESY experiments were obtained with mixing times of 100 ms. Chemical shifts were measured at 298 K in D<sub>2</sub>O.

## 4. Conclusions

In this work, for the first time, we have characterised the complete structure of the core oligosaccharide from *E. amylovora* strain CFBP1430 LPS (Scheme 5, structure 5). To this aim, we prepared three mutants, i.e. *waaL*, *wabH*, and *wabG*, the purified lipopolysaccharides of which were characterised. The reported data showed that the core oligosaccharides here reported share structural fragments with those of *Klebsiella pneumoniae* and *Serratia marcescens*. In particular, by comparison

with the core of *S. marcescens* the present structure lacks the non-stoichiometric Ko residue, a feature considered useful to distinguish between the genera *Burkholderia* and *Pseudomonas*.



**Scheme 5.** Core oligosaccharide structures from *E. amylovora* strain CFBP1430 LPS.

**Supplementary Materials:** Supplementary materials can be found at [www.mdpi.com/1422-0067/18/3/559/s1](http://www.mdpi.com/1422-0067/18/3/559/s1).

**Acknowledgments:** This work was partially funded by BIO2016-80329-P from the Spanish Ministerio de Economía y Competitividad, and from Generalitat de Catalunya (Centre de Referència en Biotecnologia). We thank Maite Polo for her technical assistance and the Servicios Científico-Técnicos from the University of Barcelona.

**Author Contributions:** Angela Casillo: Performed the experiments, suggested critical parameters in design of experiments and co-wrote the paper. Marcello Ziaco and Buko Lindner: Performed the experiments and co-wrote the paper. Susana Merino and Elena Mendoza-Barberá: Performed the experiments. Juan M. Tomás and Maria Michela Corsaro: Designed the experiments, provided advice in performance of experiments and wrote the paper.

**Conflicts of Interest:** The authors declare no conflict of interest.

## References

- Oh, C.; Beer, S.V. Molecular genetics of *Erwinia amylovora* involved in the development of fire blight. *FEMS Microbiol. Lett.* **2005**, *253*, 185–192. [[CrossRef](#)] [[PubMed](#)]
- Thomson, S.V. Epidemiology of Fire Blight. In *Fire Blight: The Disease and Its Causative Agent, Erwinia Amylovora*; Vanneste, J.L., Ed.; CABI: New York, NY, USA, 2000; pp. 9–36.
- Bellemann, P.; Geider, K. Localization of transposon insertions in pathogenicity mutants of *Erwinia amylovora* and their biochemical characterization. *J. Gen. Microbiol.* **1992**, *138*, 931–940. [[CrossRef](#)] [[PubMed](#)]
- Koczan, J.M.; McGrath, M.J.; Zhao, Y.; Sundin, G.W. Contribution of *Erwinia amylovora* exopolysaccharides amylovoran and levan to biofilm formation: Implications in pathogenicity. *Phytopathology* **2009**, *99*, 1237–1244. [[CrossRef](#)] [[PubMed](#)]
- Wilkinson, S.C. Composition and Structure of Bacterial Lipopolysaccharides. In *Surface Carbohydrates of the Prokaryotic Cell*; Sutherland, I.W., Ed.; Academic Press Inc.: New York, NY, USA, 1977; pp. 97–105.
- Lüderitz, O.; Freudenberg, M.A.; Galanos, C.; Lehmann, V.; Rietschel, E.T.; Shaw, D.H. Lipopolysaccharides of Gram-Negative Bacteria. In *Current Topics in Membranes and Transport*; Razin, S., Rottem, S., Eds.; Academic Press Inc.: New York, NY, USA, 1982; pp. 79–151.
- Westphal, O.; Lüderitz, O.; Galanos, C.; Mayer, H.; Rietschel, E.T. The Story of Bacterial Endotoxin. In *Advances in Immunopharmacology*; Chedid, L., Hadden, J.W., Spreafico, F., Eds.; Pergamon Press: Oxford, UK, 1986; pp. 13–34.
- Carillo, S.; Pieretti, G.; Bedini, E.; Parrilli, M.; Lanzetta, R.; Corsaro, M.M. Structural investigation of the antagonist LPS from the cyanobacterium *Oscillatoria planktothrix* FP1. *Carbohydr. Res.* **2014**, *388*, 73–80. [[CrossRef](#)] [[PubMed](#)]
- Alexander, C.; Rietschel, E.T. Invited review: Bacterial lipopolysaccharides and innate immunity. *J. Endotoxin Res.* **2001**, *7*, 167–202. [[CrossRef](#)] [[PubMed](#)]
- Caroff, M.; Karibian, D. Structure of bacterial lipopolysaccharides. *Carbohydr. Res.* **2003**, *338*, 2431–2447. [[CrossRef](#)] [[PubMed](#)]
- Lüderitz, O.; Galanos, C.; Risse, H.J.; Ruschmann, E.; Schlecht, S.; Schmidt, G.; Schulte-Holthausen, H.; Wheat, R.; Westphal, O.; Schlosshardt, J. Structural relationship of *Salmonella* O and R antigens. *Ann. N. Y. Acad. Sci.* **1966**, *133*, 349–374. [[CrossRef](#)] [[PubMed](#)]
- Berry, M.C.; McGhee, G.C.; Zhao, Y.; Sundin, G.W. Effect of a *waaL* mutation on lipopolysaccharide composition, oxidative stress survival, and virulence in *Erwinia amylovora*. *FEMS Microbiol. Lett.* **2009**, *291*, 80–87. [[CrossRef](#)] [[PubMed](#)]

13. Kao, C.C.; Sequeira, L. A gene cluster required for coordinated biosynthesis of lipopolysaccharide and extracellular polysaccharide also affects virulence of *Pseudomonas solanacearum*. *J. Bacteriol.* **1991**, *173*, 7841–7847. [[CrossRef](#)] [[PubMed](#)]
14. Toth, I.K.; Thorpe, C.J.; Bentley, S.D.; Mulholland, V.; Hyman, L.J.; Perombelon, M.C.M.; Salmond, G.P.C. Mutation in a gene required for lipopolysaccharide and enterobacterial common antigen biosynthesis affects virulence in the plant pathogen *Erwinia carotovora* subsp. *atroseptica*. *Mol. Plant Microbe Interact.* **1999**, *12*, 499–507. [[CrossRef](#)] [[PubMed](#)]
15. Aquilini, E.; Tomás, J.M. Lipopolysaccharides (Endotoxins). *Ref. Modul. Biomed. Sci.* **2015**. [[CrossRef](#)]
16. Pieretti, G.; Corsaro, M.M.; Lanzetta, R.; Parrilli, M.; Canals, R.; Merino, S.; Tomás, J.M. Structural studies of the O-chain polysaccharide from *Plesiomonas shigelloides* strain 302–73 (serotype O1). *Eur. J. Org. Chem.* **2008**, *2008*, 3149–3155. [[CrossRef](#)]
17. Regué, M.; Izquierdo, L.; Fresno, S.; Piqué, N.; Corsaro, M.M.; Naldi, T.; de Castro, C.; Waidelich, D.; Merino, S.; Tomas, J. A second outer-core region in *Klebsiella pneumoniae* lipopolysaccharide. *J. Bacteriol.* **2005**, *187*, 4198–4206. [[CrossRef](#)] [[PubMed](#)]
18. Holst, O.; Muller-Leonnies, S.; Lindner, B.; Brade, H. Chemical structure of the lipid A of *Escherichia coli* J-5. *Eur. J. Biochem.* **1993**, *214*, 695–701. [[CrossRef](#)] [[PubMed](#)]
19. Vinogradov, E.; Lindner, B.; Seltmann, G.; Radziejewska-Lebrecht, J.; Holst, O. Lipopolysaccharides from *Serratia marcescens* possess one or two 4-Amino-4-deoxy-L-arabinopyranose 1-phosphate residues in the Lipid A and D-glycero-D-talo-Oct-2-ulopyranosonic Acid in the inner core region. *Chem. Eur. J.* **2006**, *12*, 6692–6700. [[CrossRef](#)] [[PubMed](#)]
20. Süsskind, M.; Brade, L.; Brade, H.; Holst, O. Identification of a novel heptoglycan of  $\alpha$ 1→2-linked D-glycero-D-manno-heptopyranose. *J. Biol. Chem.* **1998**, *273*, 7006–7017. [[PubMed](#)]
21. Galanos, C.; Lüderitz, O.; Westphal, O. A new method for the extraction of R lipopolysaccharides. *Eur. J. Biochem.* **1969**, *9*, 245–249. [[CrossRef](#)] [[PubMed](#)]
22. Leontein, K.; Lindberg, B.; Lönngren, J. Assignment of absolute configuration of sugars by GLC of their acetylated glycosides formed from chiral alcohols. *Carbohydr. Res.* **1978**, *62*, 359–362. [[CrossRef](#)]
23. Holst, O. Deacylation of Lipopolysaccharides and Isolation of Oligosaccharide Phosphates, In *Bacterial Toxins: Methods and Protocols. Methods Mol. Biol.* **2000**, *145*, 345–353. [[PubMed](#)]
24. Ciucanu, I.; Kerek, F. A simple and rapid method for the permethylation of carbohydrates. *Carbohydr. Res.* **1984**, *131*, 209–217.
25. Corsaro, M.M.; Pieretti, G.; Lindner, B.; Lanzetta, R.; Parrilli, E.; Tutino, M.L.; Parrilli, M. Highly phosphorylated core oligosaccharide structures from cold-adapted *Psychromonas arctica*. *Chem. Eur. J.* **2008**, *14*, 9368–9376. [[CrossRef](#)] [[PubMed](#)]

